Dispersive determinations of lattice muon g-2 HVP quantities

Kim Maltman, York University (and CSSM, Adelaide)

with G. Benton, D. Boito, M. Golterman, A. Keshavarzi, S. Peris

DB, MG, KM, SP: *PRD105 (2022) 093003 [2203.05070 [hep-ph]]; PRD107 (2023) 034512 [2210.13677 [hep-ph]]; PRD107 (2023) 074001 [2211.11055 [hep-ph]]*

GB, DB, MG, AK, KM, SP: *PRL131 (2023) 251803 [2306.16808 [hep-ph]]; PRD109 (2024) 036010 [2311.09523 [hep-ph]]; PRD111 (2025) 034018 [2411.06637 [hep-ph]]*

CONTEXT: Pre-FNAL E989 runs 4-6 c.f. SM 2020/2025 g-2 Theory Initiative White Paper assessments

a_μ^{SM} expectations c.f. experiment: WP20 w/ dispersive HVP, WP25 w/lattice HVP

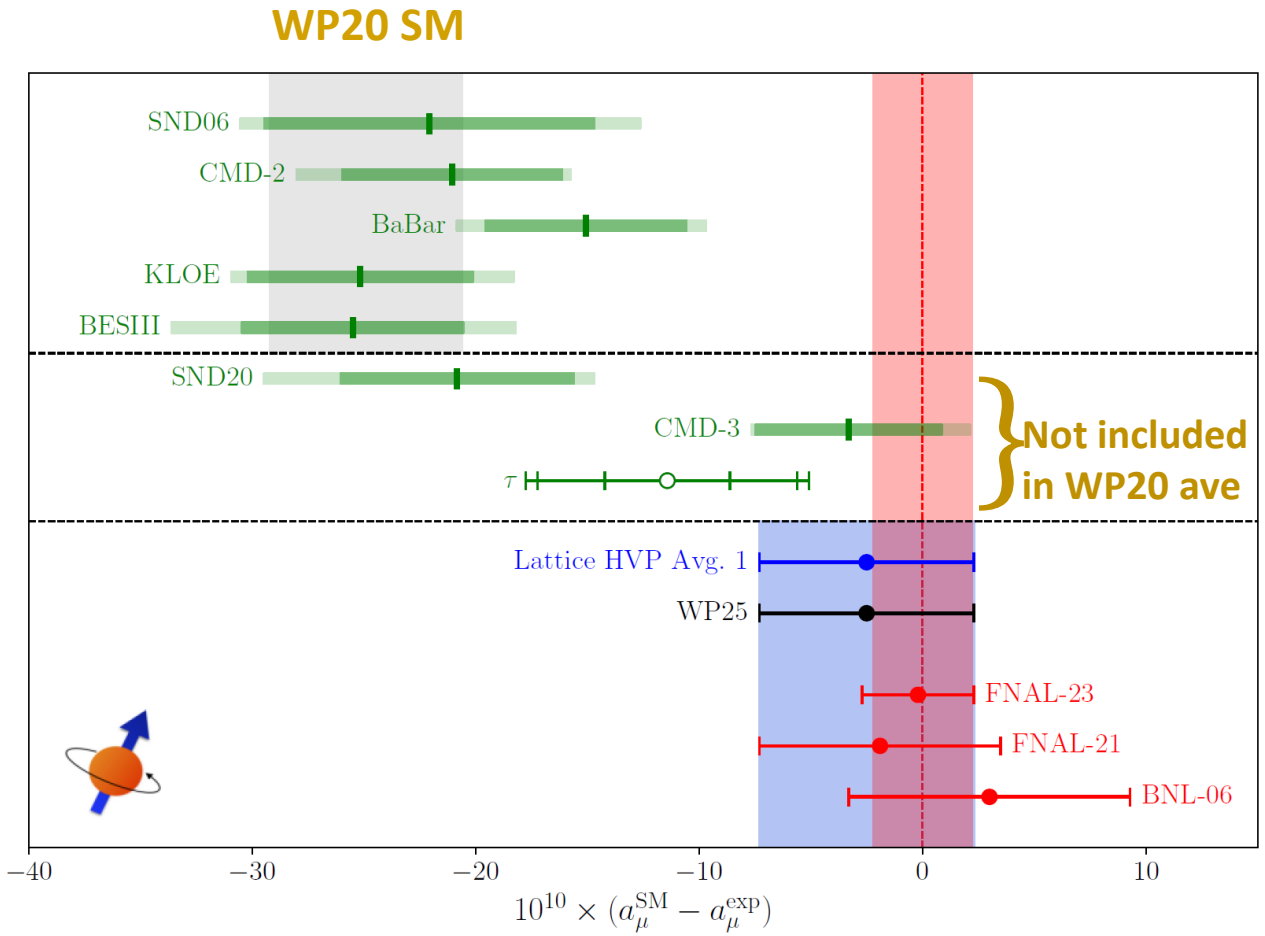

Fig. 40, WP25 [arXiv:2505.21476 [hep-ph]]

- **LHS: Grey band**: WP20 (dispersive HVP average input)
- **LHS: Blue band:** WP25 (lattice HVP average input)
- **LHS: Red band:** pre-June 3/25 experimental WA

c.f. WP20 lattice vs dispersive situation

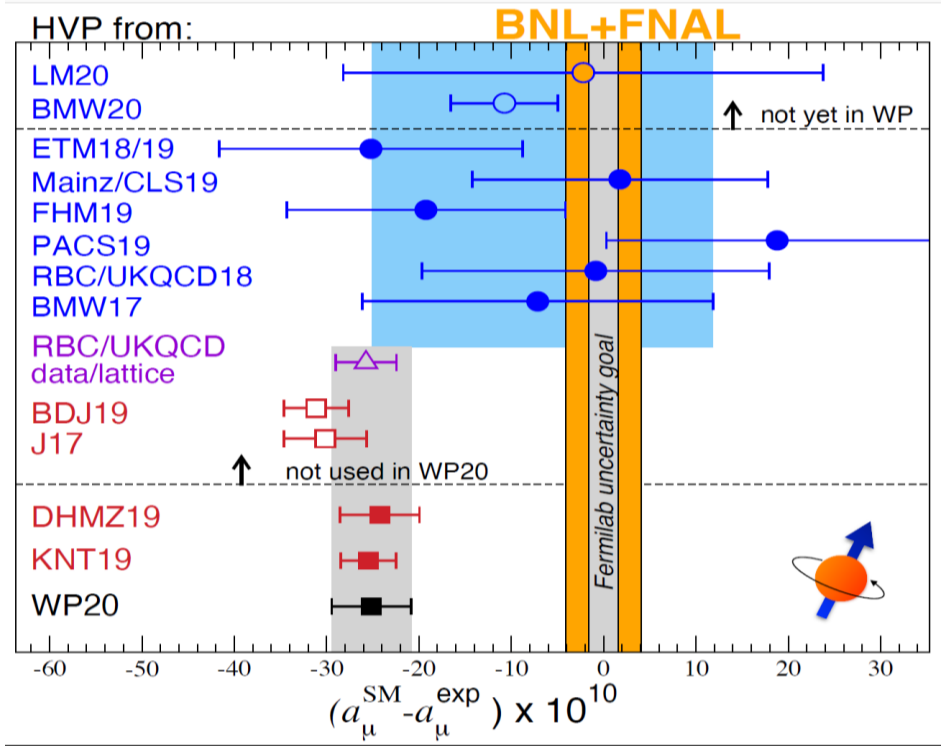

CONTEXT: Post-FNAL-E989 runs 4-6 c.f. SM 2020/2025 g-2 Theory Initiative White Paper assessments

a_μ^{SM} expectations c.f. experiment: post-June 3, 2025 FNAL E989 update

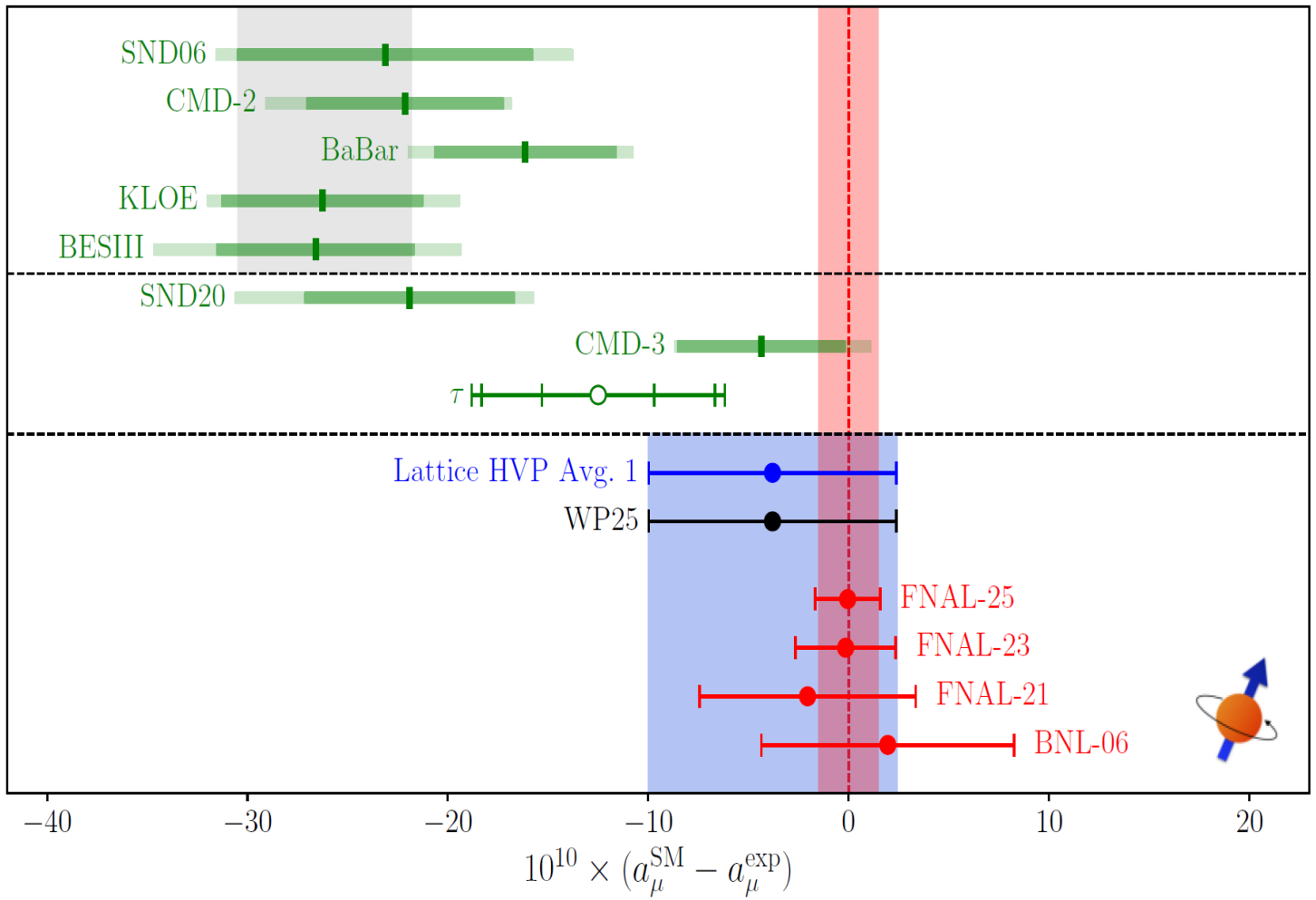

- **GREY BAND**: WP20 SM (dispersive HVP average input)
- **BLUE BAND:** WP25 SM (lattice HVP average input)
- **RED BAND:** post-June 3, 2025 experimental WA, including FNAL E989 runs 4-6

Fig. 40, WP25 [arXiv:2505.21476v2 [hep-ph]]

CONTEXT: post-WP20 lattice c.f. WP20-input dispersive for RBC/UKQCD "lqc W1 window"

Isospin limit, light-quark connected intermediate (W1) window $a_\mu^{W1,lqc}$ results

BBGKMP23: PRL 131 (2023) 251803 with KNT19 dispersive input

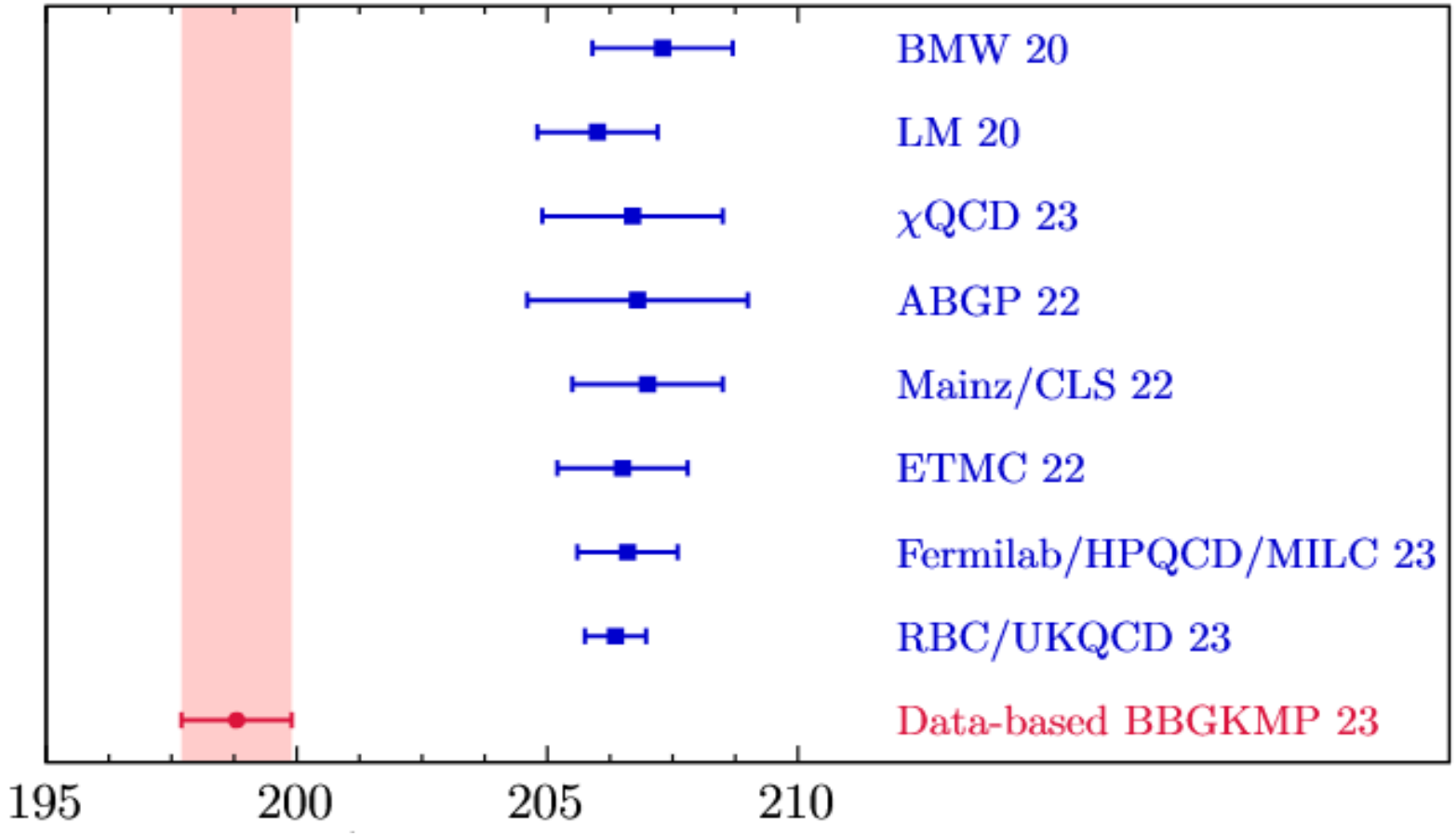

DISPERSIVE SPECTRAL AND LATTICE TIME-MOMENTUM a_μ^{HVP} REPRESENTATIONS

- **Dispersive (timelike s=q^2 spectral integral) representation:**
  - ❖ $\widehat{\Pi}(Q^2)$: Q^2=0 subtracted scalar polarization of EM current-current 2-point function
  - ❖ EM spectral function ρ(s) = Im $\widehat{\Pi}$(-s)/π, related to R-ratio by R(s) = $12\pi^2\rho$(s)

$$a_\mu^{HVP} = \frac{4\alpha^2 m_\mu^{\ 2}}{3}\int_{th}^{\infty} ds\,\frac{\hat{K}(s)}{s^2}\,\rho(s)$$

$\hat{K}$(s) known, monotically Increasing from ~0.63 at 2π threshold to 1 as s→∞

- **Lattice time-momentum (Euclidean time) integral representation:**

$$C(t) = \frac{1}{3}\sum_{i=1}^{3}\int d^3x\langle j_i^{\rm EM}(\vec{x},t) j_i^{\rm EM}(0)\rangle = \frac{1}{2}\int_{m_\pi^2}^{\infty} ds\,\sqrt{s}\,e^{-\sqrt{s}t}\,\rho_{\rm EM}(s) \quad (t>0)$$

dispersive C(t) representation

Bernecker and Meyer '11

Leading order contribution to $a_\mu^{\rm HVP}$

$$a_\mu^{\rm HVP} = 2\int_0^\infty dt\, w(t) C(t)$$

w(t) known, related to $\hat{K}$(s) by

$$\frac{\hat{K}(s)}{s^2} = \frac{3\sqrt{s}}{4\alpha^2 m_\mu^2}\int_0^\infty dt\, w(t)\, e^{-\sqrt{s}t}$$

LATTICE-MOTIVATED WINDOW QUANTITIES

- **RBC/UKQCD-style intermediate windows: reduced lattice errors by short- and long-t suppression**

$$a_\mu^W = 2\int_0^\infty dt\, f_W(t;t_0,t_1,\Delta)[w(t)C(t)] \qquad f_W(t;t_0,t_1,\Delta) = \frac{1}{2}\left(tanh\left[\frac{t-t_0}{\Delta}\right] - tanh\left[\frac{t-t_1}{\Delta}\right]\right)$$

RBC/UKQCD (W1): (t_0, t_1, Δ)=(0.4, 1.0, 0.15) fm, ABGP (W2): (t_0, t_1, Δ)=(1.5, 1.9, 0.15) fm

- **Associated short-distance (SD) and long-distance (LD) windows (HVP=SD+W+LD):**

$$f_W(t) \rightarrow f_{SD}(t) = \frac{1}{2}\left(1 - tanh\left[\frac{t-t_0}{\Delta}\right]\right) \qquad f_{LD}(t) = \frac{1}{2}\left(1 + tanh\left[\frac{t-t_1}{\Delta}\right]\right)$$

- **C(t) dispersive representation → equivalent dispersive (weighted ρ(s) integral) representations**

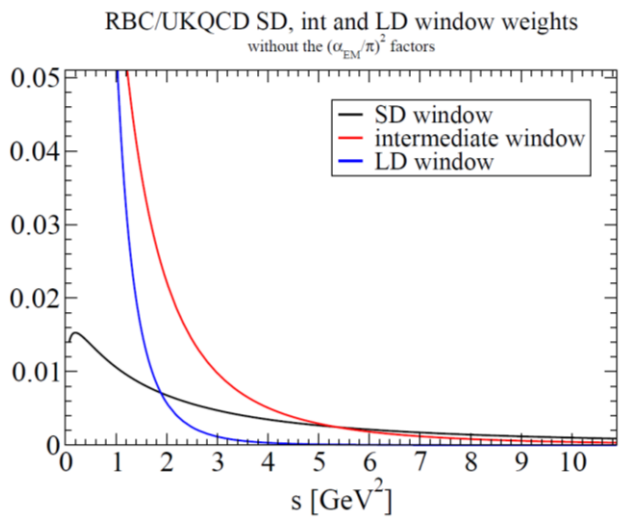

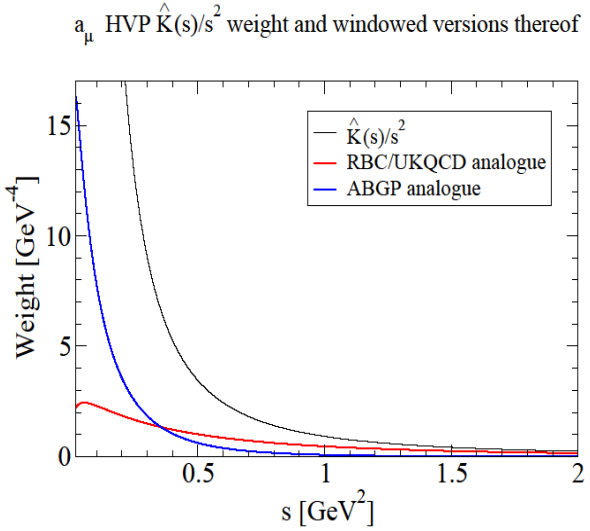

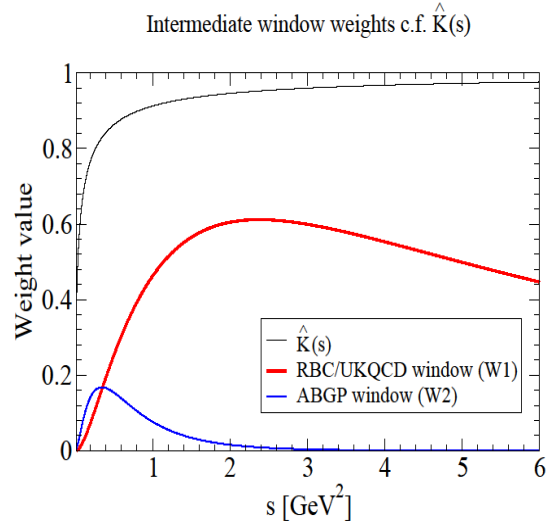

$SU(3)_F$ decompositions

$$J_\mu^{EM} = V_\mu^3 + \frac{1}{\sqrt{3}} V_\mu^8 + \cdots \equiv J_\mu^{EM,3} + J_\mu^{EM,8} + \cdots = \frac{1}{2}(\bar{u}\gamma_\mu u - \bar{d}\gamma_\mu d) + \frac{1}{6}(\bar{u}\gamma_\mu u + \bar{d}\gamma_\mu d + \bar{s}\gamma_\mu s) + \cdots$$

I=1, G-parity + I=0, G-parity -

$$\hat{\Pi}_{EM}(Q^2) = \hat{\Pi}_{EM}^{33}(Q^2) + \frac{2}{\sqrt{3}}\hat{\Pi}_{EM}^{38}(Q^2) + \frac{1}{3}\hat{\Pi}_{EM}^{88} + \cdots = \hat{\Pi}_{EM}^{I=1}(Q^2) + \hat{\Pi}_{EM}^{MI}(Q^2) + \hat{\Pi}_{EM}^{I=0}(Q^2)$$

+ similarly for $\rho_{EM}(s)$, C(t)

⇒ inherited decompositions of inclusive, exclusive-mode HVP contributions a_μ^X

$$a_\mu^X = a_\mu^{X,33} + \frac{2}{\sqrt{3}} a_\mu^{X,38} + \frac{1}{3} a_\mu^{X,88} + \cdots \equiv a_\mu^{X,I=1} + a_\mu^{X.MI} + a_\mu^{X,I=0}$$

(and analogous windowed/alternately weighted spectral integral quantities)

Isospin & quark connectedness: the "lqc" and "slqd" combinations

In the isospin limit: $\frac{1}{4}\langle(\bar{u}\gamma_\mu u - \bar{d}\gamma_\mu d)(x)(\bar{u}\gamma_\mu u - \bar{d}\gamma_\mu d)(y)\rangle = \frac{1}{2}x$ 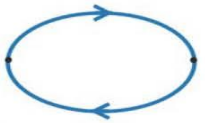 y **u, d I=1**

and $\frac{1}{36}\langle(\bar{u}\gamma_\mu u+\bar{d}\gamma_\mu d)(x)(\bar{u}\gamma_\mu u+\bar{d}\gamma_\mu d)(y)\rangle = \frac{1}{18}x$ 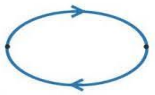 $y + \frac{1}{9}x$ 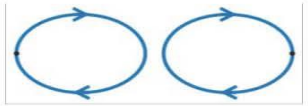 y **u, d I=0**

Therefore $R_{\rm EM}^{\rm sconn+disc} = R^{I=0} - \frac{1}{9}R^{I=1} \rightarrow R_{\rm EM}^{\rm lqc} = \frac{10}{9}R^{I=1}$

$\Rightarrow a_\mu^{W,\rm sconn+disc} = a_\mu^{W,I=0} - \frac{1}{9}a_\mu^{W,I=1} \rightarrow a_\mu^{W,\rm lqc} = \frac{10}{9}a_\mu^{W,I=1}$

slqd: strange connected+uds disconnected **lqc: light-quark connected**

Light-flavor contributions measured on the lattice

- isospin limit (IL) light-quark (u, d) connected (lqc): **in both I=0 and 1**
- IL strange-quark connected + uds disconnected (slqd) sum: **I=0 only**
- EM (connected & disconnected): **in all of I=0, I=1 and MI**
- strong isospin-breaking (SIB) (connected & disconnected): **to O(m_d-m_u): MI only**
- **Ideally: evaluate all dispersively to isolate lattice-dispersive discrepancy source(s)**

DISPERSIVE STRATEGY/INPUT FOR COMPARISONS TO LATTICE

- **Isospin limit (IL) I=0/1 separation to identify IL lqc and slqd contributions**
  - ➢ modes w/ only narrow G-parity eigenstates ($\pi, \eta, \omega, \varphi$): I=1/0 for G = +/-
  - ➢ Residual G-parity mixed ("ambiguous") modes:
    - ❖ For non-radiative modes: if no additional external input, "maximally conservative" $50 \pm 50\%\ \ I = 1,\ \ 50 \mp 50\%\ I = 0$ splits

$$\Rightarrow \quad [\rho_{\rm EM}^{\rm lqc}]_X = \left(\frac{5}{9} \pm \frac{5}{9}\right)[\rho_{\rm EM}]_X; \qquad [\rho_{\rm EM}^{\rm s+lqd}]_X = \left(\frac{4}{9} \pm \frac{5}{9}\right)[\rho_{\rm EM}]_X.$$

(and similarly for lqc, slqd windows quantities)

    - ❖ "Maximally conservative" split errors too large for largest ambiguous mode ($K\bar{K}$) contribution: crucial role of $K\bar{K}$ I=1 part of I=0+1 EM total from BaBar 2018 $\tau^- \to K^- K^0 \nu_\tau$ via CVC
    - ❖ I=0/1 $K\bar{K}\pi$ separation from BaBar 2007 Dalitz plot analysis
    - ❖ $\pi^0\gamma$, $\eta\gamma$ I=0/MI/I=1 decomposition from resonance saturation and known V=ω, φ, ρ EM decay constants, masses, widths and $V \to \pi^0\gamma$, $\eta\gamma$ widths
  - ➢ s-dependent exclusive-mode input from KNT19 to E_{CM}=1.937 GeV; pQCD (+DVs) for inclusive-region, E_{CM}>1.937 GeV, contributions

KNT19 exclusive-mode region HVP, W1 unambiguous/ambiguous-mode breakdowns

Mode(s), X	$(a_\mu^{W1})_X \times 10^{10}$	$(a_\mu^{HVP})_X \times 10^{10}$
G = + sum	168.24(72)	543.2(2.4)
G = - sum	20.69(37)	49.93(95)
$K\bar{\bar{K}}$	19.13(15)	36.07(29)
$\pi^0\gamma$	1.59(4)	4.58(10)
$K\bar{\bar{K}}\pi$	1.71(7)	2.71(12)
$\eta\gamma$	0.34(1)	0.70(2)
$K\bar{\bar{K}}\pi\pi$	1.18(5)	1.93(8)
Other G-ambiguous	0.07(4)	0.11(2)

External I=0/1 separation

$\tau \to K\bar{\bar{K}}\nu_\tau$ input

external PDG input

BaBar Dalitz plot input

external PDG input

- Dominant ambiguous-mode contribution from $K\bar{K}$; "maximally conservative" I=0/1 separation error too large for sub-% goal
- (As expected) strong cancellations in (G = -) - $\frac{1}{9}$(G = +) slqd combinations (lqc parts)
- Contributions from G-parity ambiguous modes with no (numerically relevant) external input improvement strongly dominated by $K\bar{K}\pi\pi$

DISPERSIVE STRATEGY/INPUT FOR COMPARISONS TO LATTICE (2): IB CORRECTIONS

- **IB corrections to G-parity-classified nominally I=1/0 contributions**
  - ➢ remove MI EM+SIB "contaminations" of nominally G=+/- unambiguous-mode contributions using data
    - ❖ Dominant ρ-ω-mixing-enhanced MI contaminations of nominally I=1/I=0 2π/3π contributions from Hoferichter et al. dispersive determinations:
      - ○ JHEP 10(2022) 032 (CHKS22); JHEP 08(2023) 08 (HHKS23); PRL131 (2023) 161905 (HCHKd23) for HVP and SD, W1, LD RBC/UKQCD windows
      - ○ private communication for ABGP W2, EWSR "windows"
    - ❖ other nominally I=0, 1 modes: no nearby thresholds, no nearby narrow resonance enhancements: O(1%) additional uncertainty estimates, added linearly
  - ➢ remove IB EM flavor 33, 88 contributions using lattice (BMW20) results
    - ❖ unlike MI case, only inclusive sums needed
    - ❖ full dispersive determination not feasible, significant cancellations of some dispersively quantifiable/threshold effects further favors use of (inclusive) lattice input

Pre-CMD-3 RESULTS: ILLUSTRATION (1): DISPERSIVE $a_\mu^{HVP,lqc}$ DETERMINATION

[including small updates of PRD107 (2023) 074001]

- **With KNT19 input:**

$$a_\mu^{HVP,lqc} = \left(\frac{10}{9}\right)\left(543.5(2.1) + 2.9(1.0) + 28.27(2) + 0.26(12)\right) + 1.57(55) - 4.21(47)$$

G-par +	*G-par ambig*	*pQCD*	*DVs*	*EM IB*	*MI IB*
95%	0.46%	5.0%		0.25%	-0.64%
				BMW 2024	CHKS22, HCHKd23

- **Full $a_\mu^{HVP,lqc}$ x 10^{10} results:**

$a_\mu^{HVP,lqc}$ = 635.8(2.6) (KNT19)

$a_\mu^{HVP,lqc}$ = 638.9(4.1) (DHMZ)

- **Tension w/ lattice (BMW20, RBCUKQCD24)**

c.f. lattice: C. Lehner Lattice2024

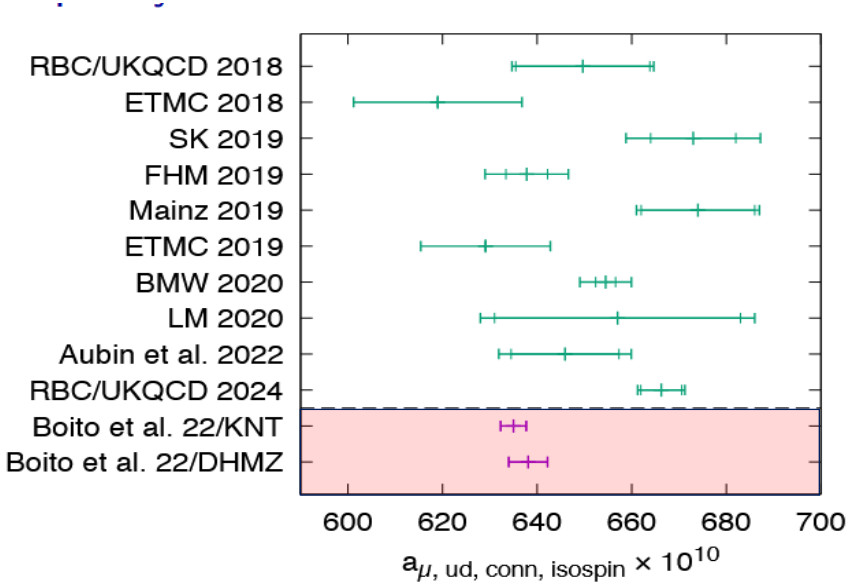

Pre-CMD-3 RESULTS: ILLUSTRATION (2): RBC/UKQCD lqc W1 WINDOW $a_\mu^{W1,lqc}$

G=+ mode X	$a_{\mu,X}^{W1}$ x 10^{10}
low-s $\pi^+\pi^-$	0.02(00)
$\pi^+\pi^-$	144.13(49)
$2\pi^+2\pi^-$	9.29(13)
$\pi^+\pi^-2\pi^0$	11.94(48)
$3\pi^+3\pi^-$ (no ω)	0.14(01)
$2\pi^+2\pi^-2\pi^0$ (no η)	0.83(11)
$\pi^+\pi^-4\pi^0$ (no η)	0.13(13)
$\eta\pi^+\pi^-$	0.85(03)
$\eta 2\pi^+2\pi^-$	0.05(01)
$\eta\pi^+\pi^-2\pi^0$	0.07(01)
$\omega(\to \pi^0\gamma)\pi^0$	0.53(01)
$\omega(\to$ npp$)3\pi$	0.10(02)
$\omega\eta\pi^0$	0.15(03)
TOTAL	168.24(72)

$a_\mu^{W1,lqc}$ contributions (in units of 10^{10})

- G=+: 186.93(80)
- $K\bar{K}$: 0.58(7)
- $K\bar{K}\pi$: 0.52(9)
- $K\bar{K}\pi\pi$: 0.60(60)
- $\pi^0\gamma$ 0.07(1)
- $\eta\gamma$ 0.06(0)
- other mixed G: 0.05(5)
- pQCD$\pm DV$s: 11.06$\pm$0.16
- EM corr'n: -0.04(6)
- 2π ($\pm$other) MI corr'n: -0.92(7)$\pm$0.29

$$a_\mu^{W1,lqc} = 199.0(1.1) \times 10^{-10}$$

G. Benton, PRL131 (2023) 251803, updated

Pre-CMD-3 RESULTS (2'): DISPERSIVE-LATTICE $a_\mu^{W1,lqc}$ COMPARISON

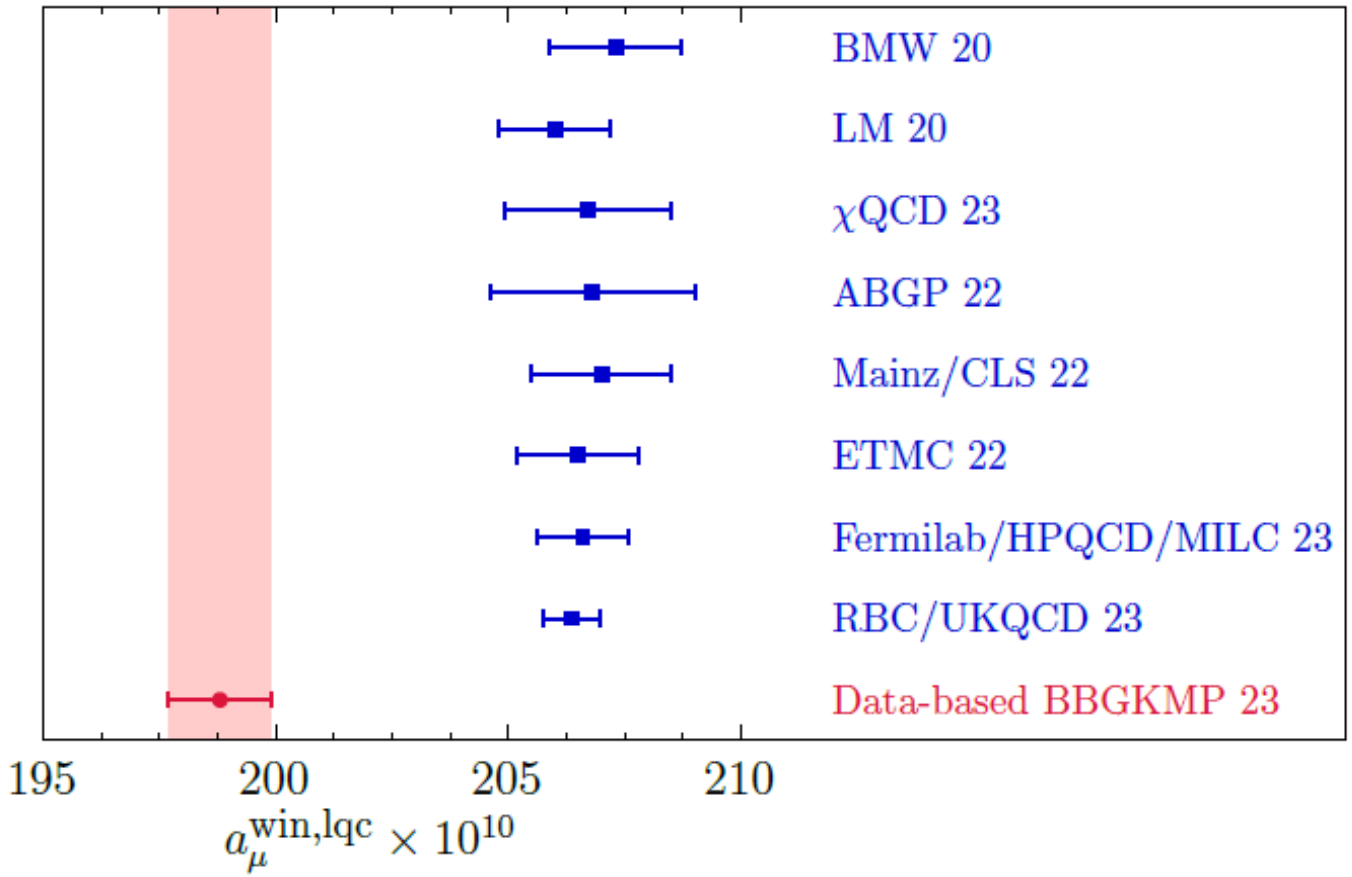

Large dispersive-lattice W1 IL, lqc discrepancy (e.g., 6σ with RBC/UKQCD 23)

Pre-CMD-3 RESULTS (3): DISPERSIVE vs LATTICE IL, slqd AND OTHER-WINDOW IL, lqc

- Lattice EM results not available for other windows: possibility 1: neglect EM I=0, 1 corrections for now (plausible based on W1 result)
- Alternates for RBC/UKQCD SD window EM error: O(α_{EM}*SD) or Mainz 2024 0.15(15)% SD_{EM}/SD result estimates
- RBC/UKQCD LD window: $LD_{EM} = HVP_{EM} – W1_{EM} - SD_{EM}$
- For IL, lqc cases, windowed versions of CHKS22 2π MI correction (from M. Hoferichter and P. Stoffer: thanks!)
- IL, slqd cases need also windowed ρ-ω region 3π MI correction of HHKS23 (provided by the authors: thanks!)
- **Compare IL dispersive and lattice results**

Pre-CMD-3 IL slqd HVP, W1 RESULTS

- **Update of PRD105 (2022) 093003 (final CHKS22 MI 2π, new HHKS23 MI 3π corrections)**
  - With KNT19 exclusive-mode contributions [Benton et al., PRD109(2024) 036010]

$$a_\mu^{HVP,slqd} \times 10^{10} = -10.43(98) + 35.13(31) + 1.89(18) + 4.00(17) + 0.94(98) + 0.11(7)$$

G-par unambig $K\bar{K}$ $K\bar{K}\pi$ $\pi^0\gamma + \eta\gamma$ $K\bar{K}\pi\pi$ other G-par ambig

$$+ 5.99(30) - 0.04(13) - [-2.68(99) - (1/9)\, 3.79(19) \pm 0.4] = 40.7(1.7)$$

pQCD±DVs I=0,1 EM MI 3π MI 2π other MI

  - With, instead, DHMZ exclusive-mode contributions: $a_\mu^{HVP,slqd} \times 10^{10}$ = **39.8(2.4)**
  - No obvious sign of discrepancy with lattice: RBC/UKQCD: 42.0(4.0); Mainz (2024): 37.3(2.4); BMW 2020: 38.0(1.8)
- **Similarly, for $a_\mu^{W1,slqd}$ x 10^{10} = 27.0(8)** [PRD109(2024) 036010] **c.f. 26.0(6) BMW2020/24**

Pre-CMD-3 DISPERSIVE RBC/UKQCD IL SD, LD WINDOW lqc, slqd RESULTS

$SD_{EM} \simeq 0 \pm (\alpha_{EM} * SD)$ or Mainz 2024 SD_{EM}/SD = 0.0015(15); $LD_{EM} = [HVP_{EM} - W1_{EM}]_{BMW20/24} - SD_{EM}$

$a_\mu^{SD,lqc} \times 10^{10} = 46.96(54)/46.89(42)$

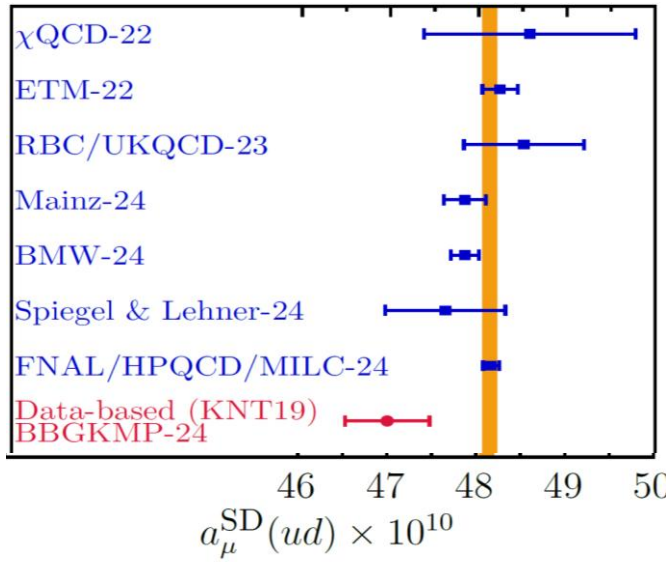

$a_\mu^{LD,lqc} \times 10^{10} = 389.9(1.7)/390.0(1.7)$

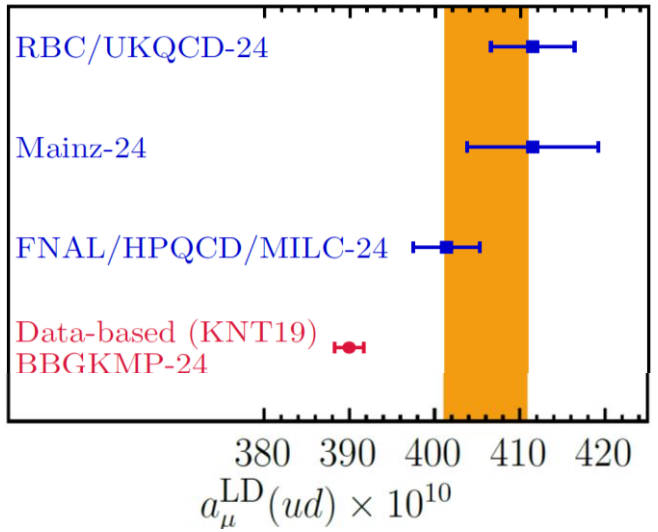

$a_\mu^{SD,slqd} \times 10^{10} = 9.21(36)$

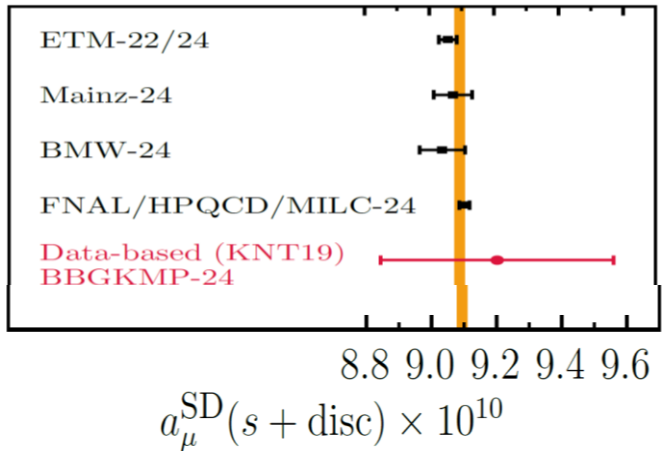

$a_\mu^{LD,slqd} \times 10^{10} = 4.53(73)$

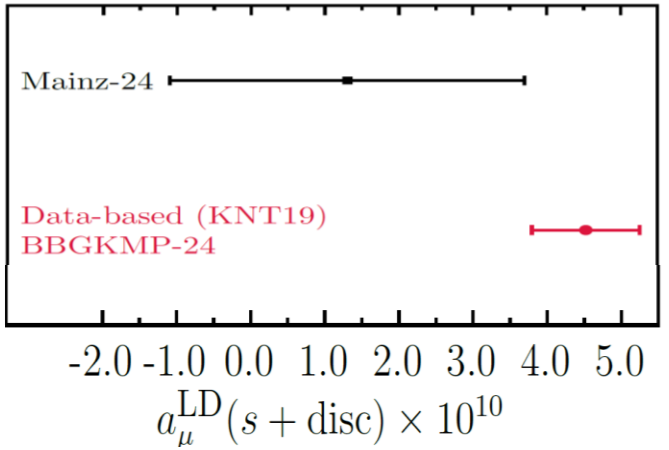

INTERIM CONCLUSIONS

- With pre-CMD-3-ππ EM R(s) data, evidence for significant dispersive-lattice discrepancies for IL, lqc HVP, RBC/UKQCD W1 and LD windows [and improved EWSR $\widehat{W}_{15}$ "window" (backup slides)]
- Pattern of discrepancies points to source in dispersive ρ region contributions
- C(t) results needed to determine a_μ^{HVP} and $a_\mu^{SD,W1,LD}$ windows and lqd, slqd components thereof also provide results for lattice sides of other RBC/UKQCD style windows and alternately weighted EWSRs (further exploration of EWSR weight choices in conjunction with new lattice data thus also of interest)
- **An obvious question still to be dealt with: the impact on the lattice-dispersive discrepancies of the new CMD-3 ππ data [PRD109(2024) 112002 [2302.08834]]?**
  - CMD-3 results too discrepant to allow combined $[\rho(s)]_{\pi\pi}$ including all experiments
  - Hence **EXPLORATORY** study with KNT19 input modified by replacement of KNT19 with CMD-3 ππ data in the region covered by CMD-3 (E_{CM}=0.33 to 1.20 GeV)

CMD-3 impact on lattice-dispersive HVP, SD, W1, LD lqc comparisons

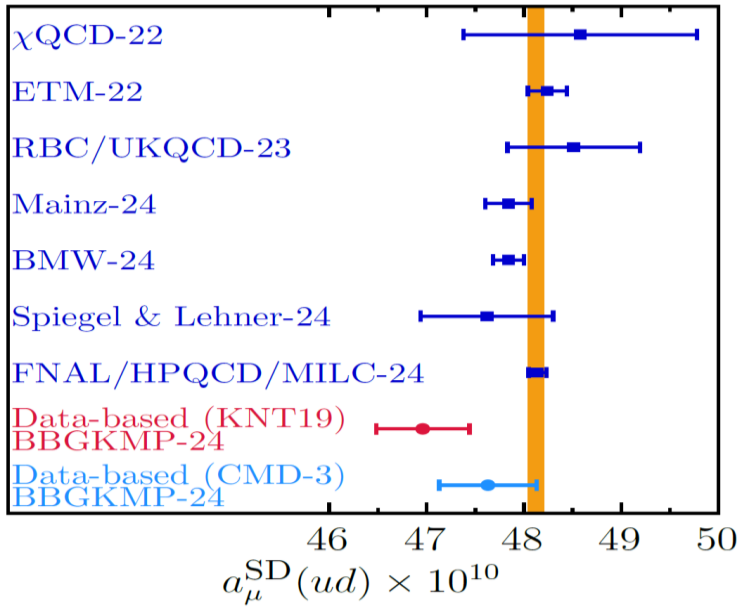

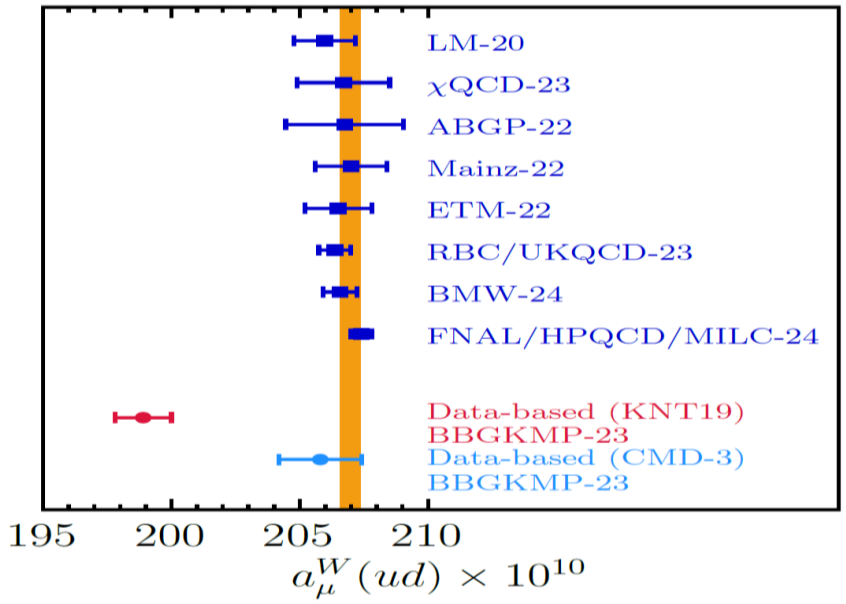

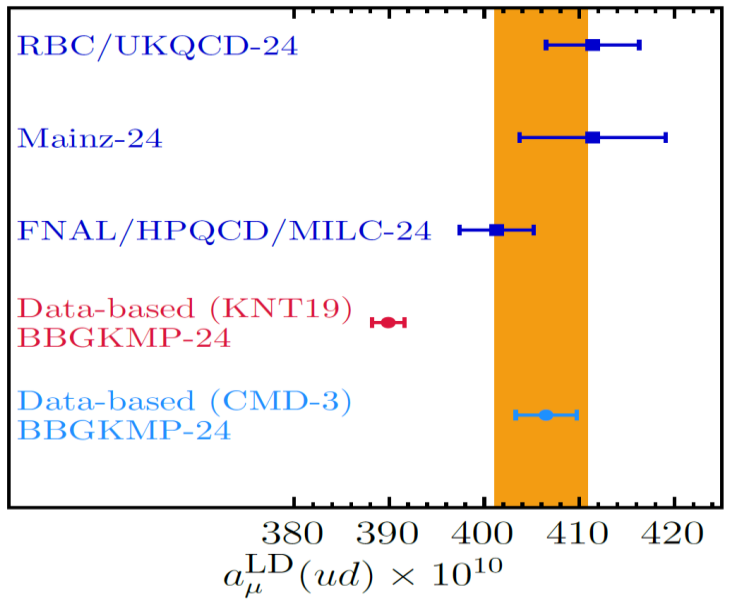

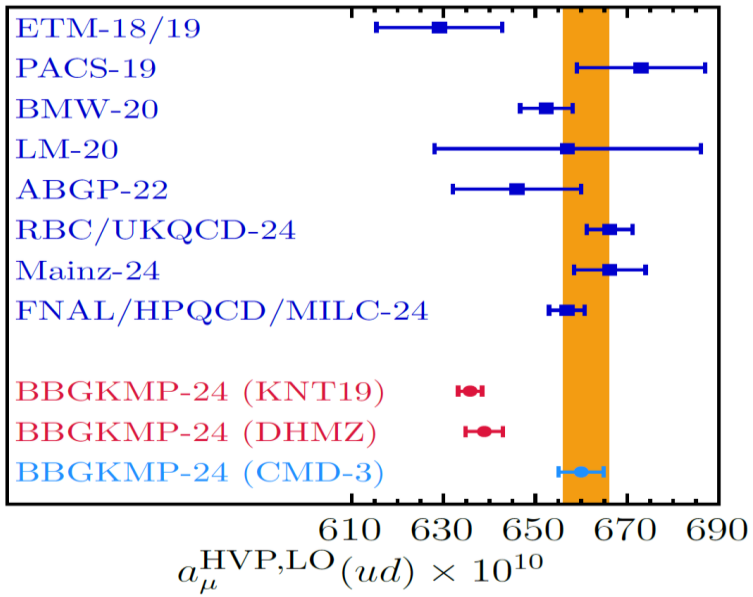

CMD-3 impact on lattice-dispersive HVP, SD, W1, LD slqd comparisons

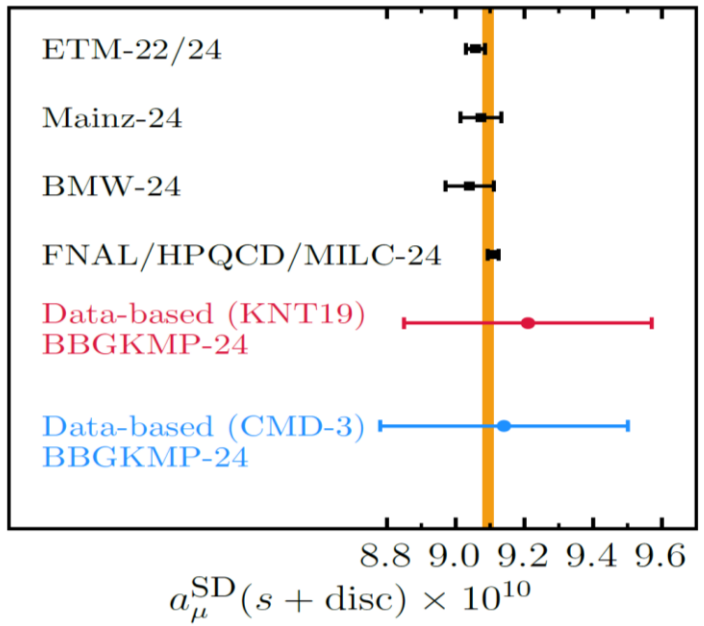

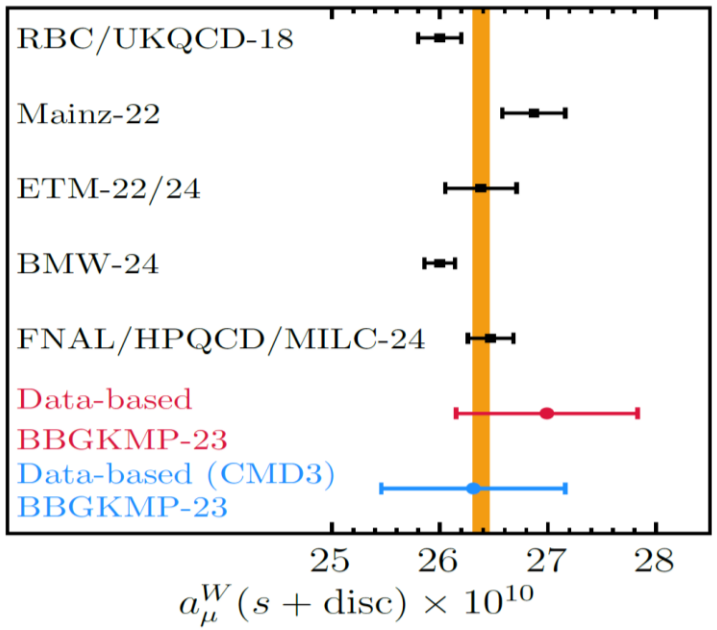

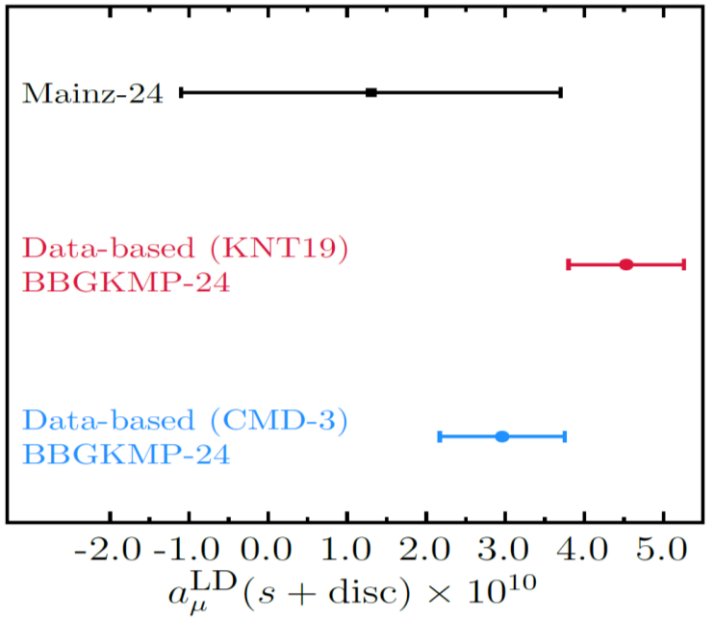

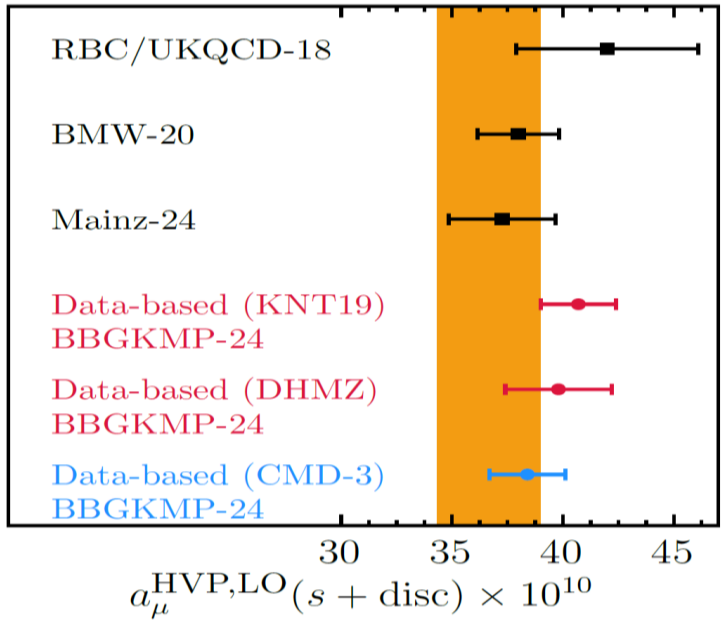

CONCLUSIONS

- Lattice and dispersive determinations of strange connected plus u,d,s disconnected HVP and window contributions all in agreement within errors
- Lattice-dispersive discrepancies for lqc HVP and several window quantities with WP20 exclusive-mode ππ cross-section dispersive input
- Discrepancies largest for quantities with largest relative ρ region dispersive contributions (HVP; W1, LD and ABGP W2 windows; EWSR "windows" tuned to emphasize ρ region)
- All observed lattice-discrepancies removed if WP20 ππ all-experiment ρ(s) contribution replaced by CMD-3 data in the $0.33 < E_{CM} < 1.20$ GeV CMD-3 region
- Some improvement possible for dispersive lqc, slqd determinations from improved low-multiplicity exclusive-mode cross section data, but $K\bar{\bar{K}}\pi\pi$ I=0/1 separation uncertainty will be an eventual limiting factor

BACKUP

EXPONENTIAL-WEIGHT-SUM-RULE "WINDOW" QUANTITIES

- **EWSR "tuned" s-dependent-weight integral quantities** [variation on Hansen, Lupo, Tantalo PRD99 (2019) 094508]
  - Choose $\{t_k\}$, tune $\{b_k\}$ to produce s-dependent weight with ~ desired shape and form

    $w(s,\{t_k\}) = \frac{1}{2}\sum_k b_k \sqrt{s}\, exp(\sqrt{s}\, t_k)$ (e.g., $\widehat{W}_{15}(s)$, $\widehat{W}_{25}(s)$ below)

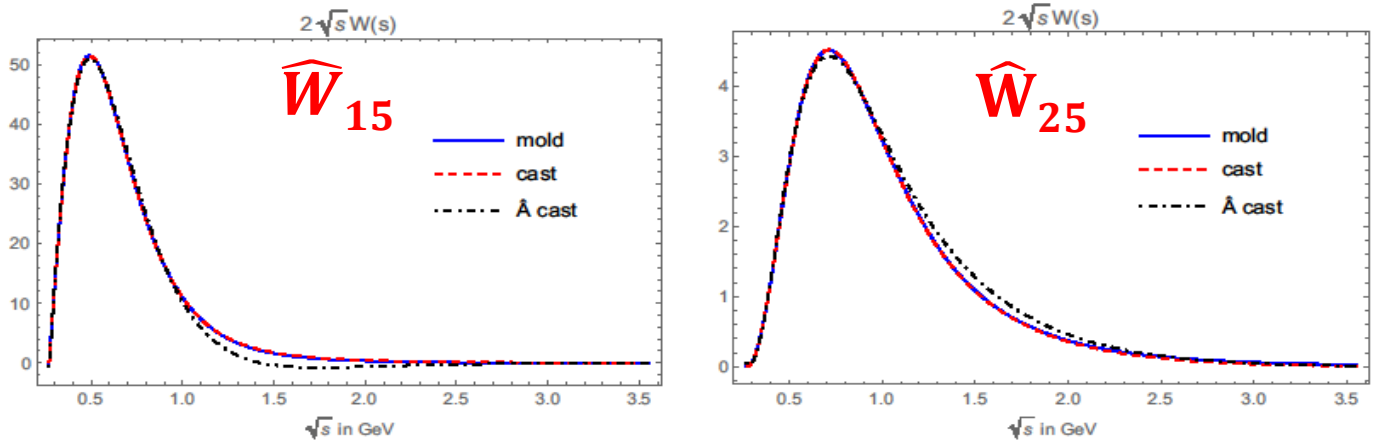

  - $\Rightarrow$ EWSR $\int_{th}^{\infty} ds\, w(s;\{t_k\})\, \rho_{EM}(s) = \sum_k b_k C(t_k)$ with tuned weight profile (in examples shown, to suppress low-s region and emphasize ρ region)
  - Restrict $\{t_k\}$ by hand to avoid large t and control lattice errors

ABGP22 INTERMEDIATE WINDOW (W2) RESULTS

- **RBC/UKQCD-style intermediate window, designed to be longer distance, more amenable to possible use of ChPT for FV** [Aubin et al. PRD106 (2022) 054503]

light-quark connected from KNT19 R(s) data

$$a_\mu^{W2,\mathrm{lqc}} = 93.70(36) \times 10^{-10}$$

Benton, et al. PRD109 (2024) 036010

Includes -0.85(4) x 10^{-10} MI IB correction

lattice results

Aubin, Blum, Golterman, Peris '22

$$a_\mu^{W2,\mathrm{lqc}} = 102.1(2.4) \times 10^{-10}$$

Fermilab/HPQCD/MILC '23

$$a_\mu^{W2,\mathrm{lqc}} = 100.7(3.2) \times 10^{-10}$$

BMW 2407.10813

$$a_\mu^{W2,lqc} = 97.67(1.62) \times 10^{-10}$$

EWSR WEIGHT ($\widehat{W}_{15}$, $\widehat{W}_{25}$) IL, lqc RESULTS

- $I_W^{lqc} \equiv \int_{th}^{\infty} ds\, W(s)\, \rho_{EM}^{IL,lqc}(s)$

lqc from KNT19 R(s) data

$$I^{\rm lqc}_{\widehat{W}_{15}} = 42.78(16) \times 10^{-2}$$
$$I^{\rm lqc}_{\widehat{W}_{25}} = 78.85(46) \times 10^{-3}$$

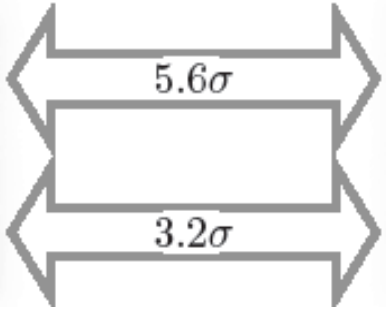

ABGP lqc lattice data

$$I^{\rm lqc}_{\hat{W}_{15}} = 46.69(68) \times 10^{-2}$$
$$I^{\rm lqc}_{\hat{W}_{25}} = 82.4(1.0) \times 10^{-3}$$

Benton, et al. PRD109 (2024) 036010

IB correction contributions:
$\widehat{W}_{15}$: -0.37 x 10^{-2}
$\widehat{W}_{25}$: -0.33 x 10^{-3}

systematic errors on lattice results still to be assessed

- **Another sign of dispersive-lattice IL, lqc ρ-region tension**

Impact of CMD-3 ππ data on IL, lqc W2, $\widehat{W}_{15}$ and $\widehat{W}_{25}$ results

- KNT19 $a_\mu^{W2,lqc}$ = 93.7(4) x10^{-10} → 97.8(8) x10^{-10} c.f. lattice 102.1(2.4)x10^{-10} (ABGP) 100.7(3.2) x10^{-10} (FHM) 97.67(1.62) x10^{-10} (BMW24) (3.5, 2.2, 2.4 σ → 1.8, 0.9, 0.1 σ)

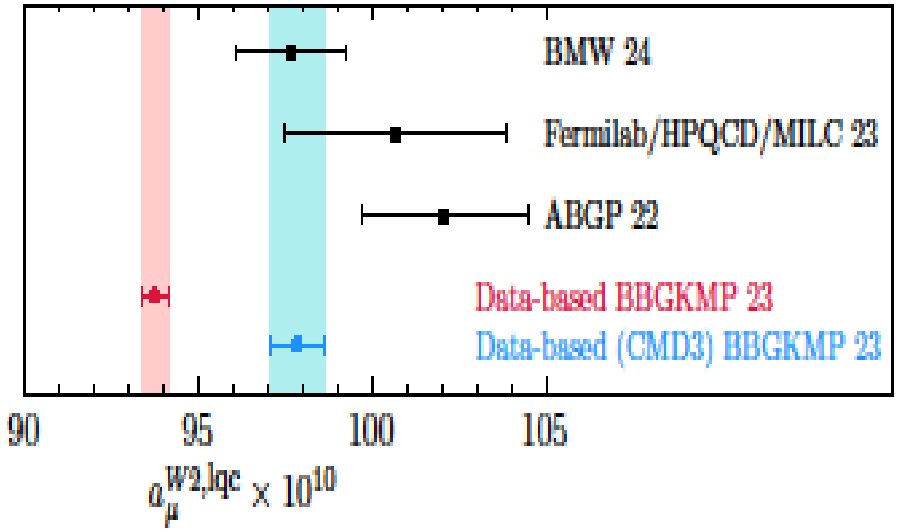

- EWSR weight discrepancies [recall, lattice errors statistical only]
  - W_{15} IL, lqc KNT19 result 0.4278(16) → 0.4483(37) c.f. lattice 0.4669(58) (5.6 σ → 2.7 σ)
  - $\widehat{W}_{25}$ IL, lqc KNT19 result 0.0789(5) → 0.0815(6) c.f. lattice 0.0824(10) (3.2 σ → 0.8 σ)
- **All dispersive-lattice differences strongly reduced with CMD-3 ππ input**

ρ-ω REGION MI EXCLUSIVE-MODE "CONTAMINATIONS"

- 2π: expect dominance by narrow, enhanced ρ-ω mixing contribution

  : dispersive evaluation (Hoferichter et al. PRL131(2023) 161905): IB ~0.7% of ππ total
- 3π: also expect dominance by ρ-ω mixing contribution

  - IC 2π ~9 x 3π a_μ^{HVP} contribution, but ~9 x natural compensating 3π to 2π IB enhancement
  - ρ-ω mixing in 2π and 3π from same s region, hence no 3π c.f.. 2π suppression from HVP weight falloff
  - Significant 2π-3π cancellation (natural opposite signs from ρ-ω mixing source)
  - Seen explicitly in Kubis et al. JHEP 08 (2023) 08 dispersive analysis

ρ-ω mixing enhancement of IB in $e^+e^- \to 3\pi$

$IC^*IB/|IC|^2 \propto g_\rho\, g_\omega / g_\rho^2 = g_\omega/g_\rho \cong 1/3$

$IC^*IB/|IC|^2 \propto g_\rho\, g_\omega / g_\omega^2 = g_\rho/g_\omega \cong 3$

DISPERSIVELY QUANTIFIABLE ENHANCED/IDENTIFIABLE EXCLUSIVE-MODE IB CONTRIBUTIONS

[Hoferichter et al. PRL131(2023) 161905 [2307.02532]]

	SD		int		LD		full		Main source
	$\mathcal{O}(e^2)$	$\mathcal{O}(\delta)$	$\mathcal{O}(e^2)$	$\mathcal{O}(\delta)$	$\mathcal{O}(e^2)$	$\mathcal{O}(\delta)$	$\mathcal{O}(e^2)$	$\mathcal{O}(\delta)$	
$\pi^0\gamma$	0.16(0)	–	1.52(2)	–	2.70(4)	–	4.38(6)	–	EM 88 (38, 33)
$\eta\gamma$	0.05(0)	–	0.34(1)	–	0.31(1)	–	0.70(2)	–	EM 88 (38, 33)
$\omega(\to \pi^0\gamma)\pi^0$	0.15(0)	–	0.54(1)	–	0.19(0)	–	0.88(2)	–	EM 33
FSR (2π)	0.12(0)	–	1.17(1)	–	3.13(3)	–	4.42(4)	–	EM 33
FSR (3π)	0.03(0)	–	0.20(0)	–	0.28(1)	–	0.51(1)	–	EM 88
FSR (K^+K^-)	0.07(0)	–	0.39(2)	–	0.29(2)	–	0.75(4)	–	EM 88 (38, 33)
ρ–ω mixing (2π)	–	0.06(1)	–	0.86(6)	–	2.87(12)	–	3.79(19)	SIB (+EM) 38
ρ–ω mixing (3π)	–	−0.13(3)	–	−1.03(27)	–	−1.52(40)	–	−2.68(70)	SIB (+EM) 38
pion mass (2π)	0.04(8)	–	−0.09(56)	–	−7.62(63)	–	−7.67(94)	–	EM 33
kaon mass (K^+K^-)	−0.29(1)	0.44(2)	−1.71(9)	2.63(14)	−1.24(6)	1.91(10)	−3.24(17)	4.98(26)	EM 88 (+SIB 38)
kaon mass $(\bar{K}^0K^0)$	0.00(0)	−0.41(2)	−0.01(0)	−2.44(12)	−0.01(0)	−1.78(9)	−0.02(0)	−4.62(23)	
sum	0.33(8)	−0.04(4)	2.34(57)	0.02(33)	−1.97(63)	1.48(44)	0.71(95)	1.47(80)	

- Exclusive EM 33, 88: subsumed into EM 33, 88 inclusive totals
- SIB (+EM) 38 needed in exclusive-mode form to remove nominal I=1, 0 MI contaminations
- Note: significant cancellation in most sums (advantage for inclusive lattice determination)

VARIATION OF ππ DISPERSIVE OUTPUT WITH ANALYSIS INPUT DETAILS

Contributions to E_{CM}=1.8 GeV, with WP20 input for regions not covered by given experiment
[percentages: those from data from the given experiment itself]

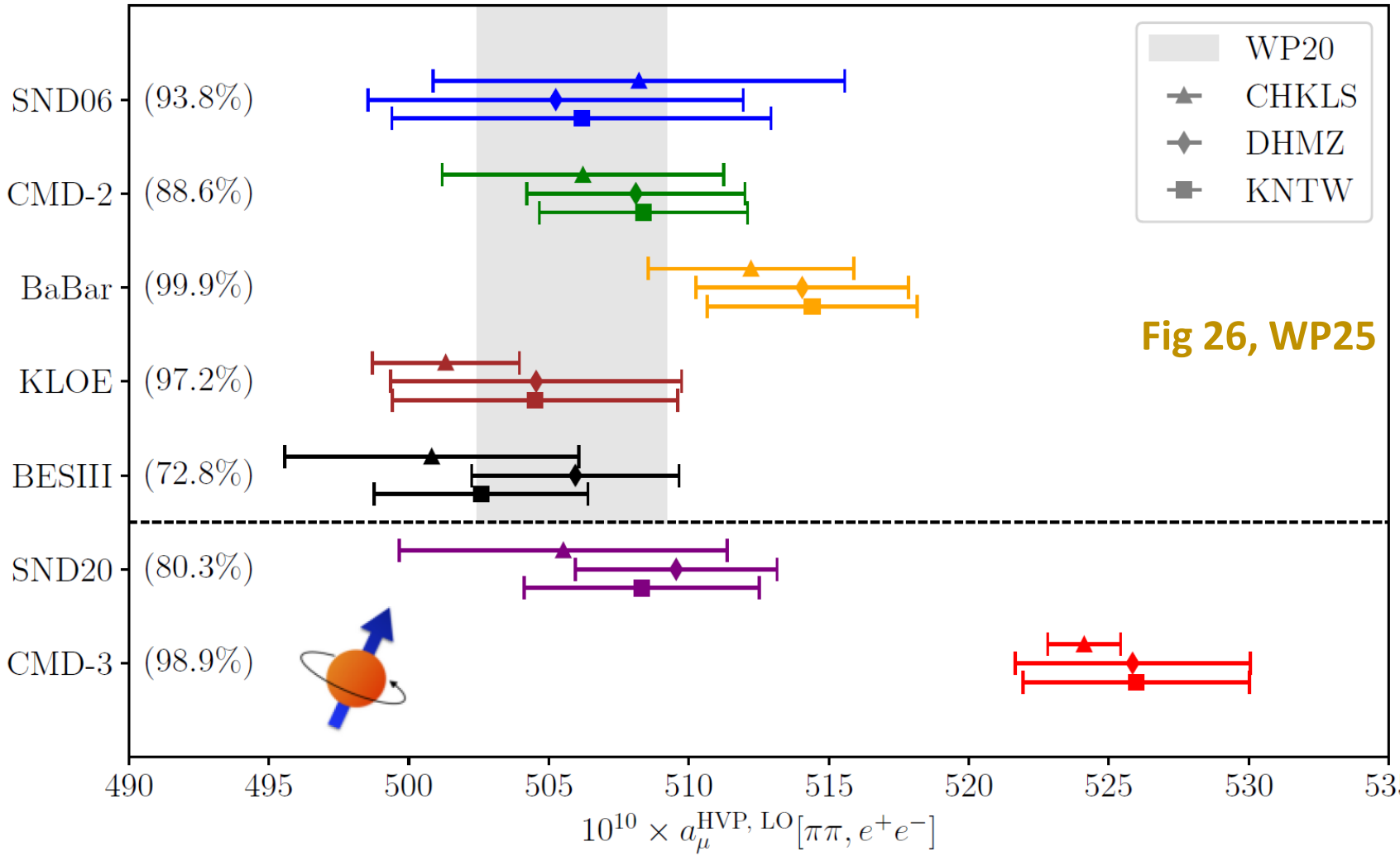

Fig 26, WP25